1

Nonlinear circuit design methods

This chapter presents the most commonly used design techniques for analysing nonlinear circuits, in particular, transistor oscillators. There are several approaches to analyse and design nonlinear circuits, depending on their main specifications. This means an analysis both in the time domain to determine transient circuit behaviour and in the frequency domain to improve power and spectral performances when parasitic effects such as instability and spurious emission must be eliminated or minimized. Using the time-domain technique, it is relatively easy to describe a nonlinear circuit with differential equations, which can be solved analytically in explicit form for only a few simple cases. Under an assumption of slowly varying amplitude and phase, it is possible to obtain separate truncated first-order differential equations for the amplitude and phase of the oscillation process from the original second-order nonlinear differential equation. However, generally it is required to use numerical methods. The time-domain analysis is limited to its inability to operate with the circuit immittance (impedance or admittance) parameters as well as the fact that it can be practically applied only for circuits with lumped parameters or ideal transmission lines. The frequency-domain analysis is less ambiguous because a relatively complex circuit can often be reduced to one or more sets of immittances at each harmonic component. For example, using a quasilinear approach, the nonlinear circuit parameters averaged by fundamental component allow one to apply a linear circuit analysis. Advanced modern CAD simulators incorporate both time-domain and frequency-domain methods as well as optimization techniques to provide all necessary design cycles.

This chapter also includes a brief introduction of simulator tools based on the Ansoft Serenade circuit simulator. In addition, some practical equations, such as the Taylor and Fourier series expansions, Bessel functions, trigonometric identities and the concept of the conduction angle, which simplify the circuit design procedure, are given.

COPYRIGHTED MATERIAL

1.1 SPECTRAL-DOMAIN ANALYSIS

The best way to understand the oscillator electrical behaviour and the fastest way to calculate its basic electrical characteristics such as output power, efficiency, phase noise, or harmonic suppression, is to use a spectral-domain analysis. Generally, such an analysis is based on the determination of the output response of the nonlinear active device when the multiharmonic

RF and Microwave Transistor Oscillator Design A. Grebennikov
© 2007 John Wiley & Sons, Ltd

signal is applied to its input port, which analytically can be written in the form

$$i(t) = f[v(t)] \tag{1.1}$$

where $i(t)$ is the output current, $v(t)$ is the input voltage and $f(v)$ is the nonlinear transfer function of the device. Unlike the spectral-domain analysis, time-domain analysis establishes the relationships between voltage and current in each circuit element in the time domain when a system of nonlinear integrodifferential equations is obtained applying Kirchhoff's law to the circuit to be analysed.

The voltage $v(t)$ in frequency domain generally represents the multiple frequency signal at the device input in the form

$$v(t) = V_0 + \sum_{k=1}^{N} V_k \cos(\omega_k t + \phi_k) \tag{1.2}$$

where V_0 is the constant voltage, V_k is the voltage amplitude and ϕ_k is the phase of the kth-order harmonic component ω_k, $k = 1, 2, \ldots, N$, and N is the number of harmonics.

The spectral domain analysis based on substituting Equation (1.2) in Equation (1.1) for a particular nonlinear transfer function of the active device determines an output spectrum as a sum of the fundamental-frequency and higher-order harmonic components, the amplitudes and phases of which will determine the output signal spectrum. Generally, this is a complicated procedure which requires a harmonic balance technique to numerically calculate an accurate nonlinear circuit response. However, the solution can be found analytically in a simple way when it is necessary to estimate only the basic performance of on oscillator in the form of the output power and efficiency. In this case, a technique based on a piecewise-linear approximation of the device transfer function can provide a clear insight into the basic oscillator behaviour and its operation modes. It can also serve as a good starting point for a final computer-aided design and optimization procedure.

The result of the spectral-domain analysis is shown as a summation of the harmonic components, the amplitudes and phases of which will determine the output signal spectrum. This problem can be solved analytically by using trigonometric identities, piecewise-linear approximation or Bessel functions.

1.1.1 Trigonometric identities

The use of trigonometric identities is very convenient when the transfer characteristic of the nonlinear element can be represented by the power series

$$i = a_0 + a_1 v + a_2 v^2 + \ldots + a_n v^n \tag{1.3}$$

If the effect of the input signal represents a single harmonic oscillation in the form

$$v = V \cos(\omega t + \phi) \tag{1.4}$$

then, by substituting Equation (1.4) into Equation (1.3), the power series can be written as

$$i = a_0 + a_1 V \cos(\omega t + \phi) + a_2 V^2 \cos^2(\omega t + \phi) + \ldots + a_n V^n \cos^n(\omega t + \phi) \tag{1.5}$$

To represent the right-hand side of Equation (1.5) as a sum of first-order cosine components, the following trigonometric identities, which replace the nth-order cosine components, can be used:

$$\cos^2\psi = \frac{1}{2}(1 + \cos 2\psi) \tag{1.6}$$

$$\cos^3\psi = \frac{1}{4}(3\cos\psi + \cos 3\psi) \tag{1.7}$$

$$\cos^4\psi = \frac{1}{8}(3 + 4\cos 2\psi + \cos 4\psi) \tag{1.8}$$

$$\cos^5\psi = \frac{1}{16}(10\cos\psi + 5\cos 3\psi + \cos 5\psi) \tag{1.9}$$

where $\psi = \omega t + \phi$.

By using the appropriate substitutions from Equations (1.6–1.9) and equating the signal frequency component terms, Equation (1.5) can be rewritten as

$$i = I_0 + I_1\cos(\omega t + \phi) + I_2\cos 2(\omega t + \phi) + I_3\cos 3(\omega t + \phi) + \ldots + I_n\cos n(\omega t + \phi) \tag{1.10}$$

where

$$I_0 = a_0 + \frac{1}{2}a_2V^2 + \frac{3}{8}a_4V^4 + \ldots$$

$$I_1 = a_1V + \frac{3}{4}a_3V^3 + \frac{5}{8}a_5V^5 + \ldots$$

$$I_2 = \frac{1}{2}a_2V^2 + \frac{1}{2}a_4V^4 + \ldots$$

$$I_3 = \frac{1}{4}a_3V^3 + \frac{5}{16}a_5V^5 + \ldots$$

Comparing Equations (1.3) and (1.10), we find:

- For nonlinear elements, the output spectrum contains frequency components which are multiples of the input signal frequency. The number of the highest-frequency component is equal to the maximum degree of the power series. Therefore, if it is necessary to know the amplitude of n-harmonic response, the volt–ampere characteristic of nonlinear element should be approximated by not less than an n-order power series.
- The output dc and even-order harmonic components are determined only by the even voltage degrees in the device transfer characteristic given by Equation (1.3). The odd-order harmonic components are defined only by the odd voltage degrees for the single harmonic input signal given by Equation (1.4).
- The current phase ψ_k of the kth-order harmonic component $\omega_k = k\omega$ is k times larger than the input signal current phase ψ:

$$\psi_k = \omega_k t + \phi_k = k(\omega t + \phi) \tag{1.11}$$

that is also applied to their initial phases defined as

$$\phi_k = k\phi \tag{1.12}$$

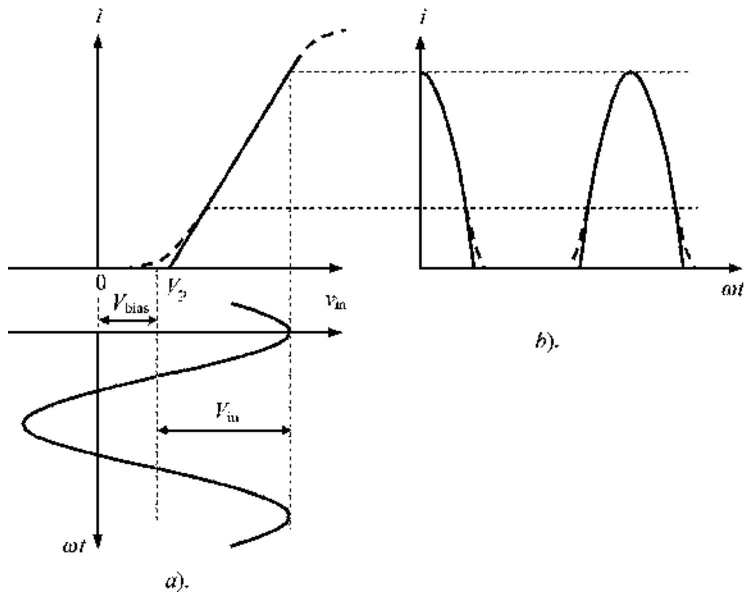

Figure 1.1 Piecewise-linear approximation technique

1.1.2 Piecewise-linear approximation

The piecewise-linear approximation of the active device current–voltage transfer characteristic is a result of replacing the actual nonlinear dependence $i = f(v_{\text{in}})$, where v_{in} the voltage applied to the device input, by an approximate one that consists of straight lines tangential to the actual dependence at the specified points. Such a piecewise-linear approximation for the case of two straight lines is shown in Figure 1.1a.

The output current waveforms for the actual current–voltage dependence (dashed curve) and its piecewise-linear approximation by two straight lines (solid curve) are plotted in Figure 1.1b. Under large-signal operation mode, the waveforms corresponding to these two dependencies are practically the same for the most part with negligible deviation for small values of the output current close to the pinch-off region of the device operation and significant deviation close to the saturation region of the device operation. However, the latter case results in a significant nonlinear distortion and is used only for high-efficiency operation modes when the active period of the device operation is minimized. Hence, at least two first output current components, dc and fundamental, can be calculated through a Fourier series expansion with a sufficient accuracy. Therefore, such a piecewise-linear approximation with two straight lines can be effective for a quick estimate of the oscillator output power and efficiency.

In this case, the piecewise-linear active device transfer current–voltage characteristic is defined by

$$i = \begin{cases} 0 & v_{\text{in}} \leq V_{\text{p}} \\ g_{\text{m}}(v_{\text{in}} - V_{\text{p}}) & v_{\text{in}} \geq V_{\text{p}} \end{cases} \tag{1.13}$$

where g_{m} is the device transconductance, V_{p} is the pinch-off voltage.

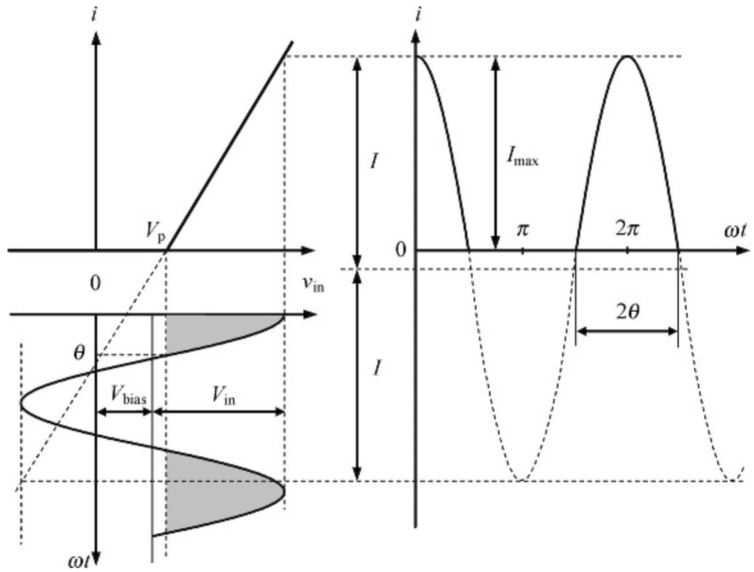

Figure 1.2 Schematic definition of conduction angle

Let us assume the input signal to be of cosinusoidal form

$$v_{in} = V_{bias} + V_{in} \cos \omega t \tag{1.14}$$

where V_{bias} is the input dc bias voltage.

At the point on the plot when voltage $v_{in}(\omega t)$ becomes equal to a pinch-off voltage V_p and where $\omega t = \theta$, the output current $i(\theta)$ has value zero. At this moment

$$V_p = V_{bias} + V_{in} \cos \theta \tag{1.15}$$

and θ can be calculated from

$$\cos \theta = -\frac{V_{bias} - V_p}{V_{in}} \tag{1.16}$$

As a result, the output current represents a periodic pulsed waveform described by the cosinusoidal pulses with the maximum amplitude I_{max} and width 2θ as

$$i = \begin{cases} I_q + I \cos \omega t & -\theta \le \omega t < \theta \\ 0 & \theta \le \omega t < 2\pi - \theta \end{cases} \tag{1.17}$$

where the conduction angle 2θ indicates the part of the RF current cycle during which device conduction occurs, as shown in Figure 1.2. When the output current $i(\omega t)$ has value zero, one can write

$$i = I_q + I \cos \theta = 0 \tag{1.18}$$

Taking into account that, for a piecewise-linear approximation, $I = g_m V_{in}$, Equation (1.17) can be rewritten as

$$i = g_m V_{in} (\cos \omega t - \cos \theta) \tag{1.19}$$

When $\omega t = 0$, then $i = I_{\max}$ and

$$I_{\max} = I(1 - \cos\theta) \tag{1.20}$$

The angle θ characterizes the class of the active device operation. If $\theta = \pi$ or 180°, the device operates in the active region during the entire period (class A operation). When $\theta = \pi/2$ or 90°, the device operates half a wave period in the active region and half a wave period in the pinch-off region (class B operation). The values of $\theta > 90°$ correspond to class AB operation with a certain value of the quiescent output current. Therefore, the double angle 2θ is called the conduction angle, the value of which directly indicates the class of the active device operation.

The Fourier series expansion of the even function when $i(t) = i(-t)$ contains only even component functions and can be written as

$$i(t) = I_0 + I_1 \cos\omega t + I_2 \cos 2\omega t + I_3 \cos 3\omega t + \ldots \tag{1.21}$$

where the dc, fundamental-frequency and nth-order harmonic components are calculated by

$$I_0 = \frac{1}{2\pi} \int_{-\theta}^{\theta} g_{\mathrm{m}} V_{\mathrm{in}} (\cos\omega t - \cos\theta)\, d(\omega t) = \gamma_0(\theta) I \tag{1.22}$$

$$I_1 = \frac{1}{\pi} \int_{-\theta}^{\theta} g_{\mathrm{m}} V_{\mathrm{in}} (\cos\omega t - \cos\theta) \cos\omega t\, d(\omega t) = \gamma_1(\theta) I \tag{1.23}$$

$$I_{\mathrm{n}} = \frac{1}{\pi} \int_{-\theta}^{\theta} g_{\mathrm{m}} V_{\mathrm{in}} (\cos\omega t - \cos\theta) \cos(n\omega t)\, d(\omega t) = \gamma_{\mathrm{n}}(\theta) I \tag{1.24}$$

where $\gamma_n(\theta)$ are called the coefficients of expansion of the output current cosinusoidal pulse or the current coefficients [1]. They can be analytically defined as

$$\gamma_0(\theta) = \frac{1}{\pi}(\sin\theta - \theta\cos\theta) \tag{1.25}$$

$$\gamma_1(\theta) = \frac{1}{\pi}\left(\theta - \frac{\sin 2\theta}{2}\right) \tag{1.26}$$

$$\gamma_n(\theta) = \frac{1}{\pi}\left[\frac{\sin(n-1)\theta}{n(n-1)} - \frac{\sin(n+1)\theta}{n(n+1)}\right] \tag{1.27}$$

where $n = 2, 3, \ldots$.

The dependencies of $\gamma_n(\theta)$ for the dc, fundamental-frequency, second- and higher-order current components are shown in Figure 1.3. The maximum value of $\gamma_n(\theta)$ is achieved when $\theta = 180°/n$. A special case is $\theta = 90°$, when odd current coefficients are equal to zero, i.e., $\gamma_3(\theta) = \gamma_5(\theta) = \ldots = 0$. The ratio between the fundamental-frequency and dc components $\gamma_1(\theta)/\gamma_0(\theta)$ varies from 1 to 2 for any values of the conduction angle, with a minimum value of 1 for $\theta = 180°$ and a maximum value of 2 for $\theta = 0°$. It is necessary to pay attention to the fact that, for example, the current coefficient $\gamma_3(\theta)$ becomes negative within the interval of $90° < \theta < 180°$. This implies appropriate phase changes of the third current harmonic component when its values are negative. Consequently, if the harmonic components for which

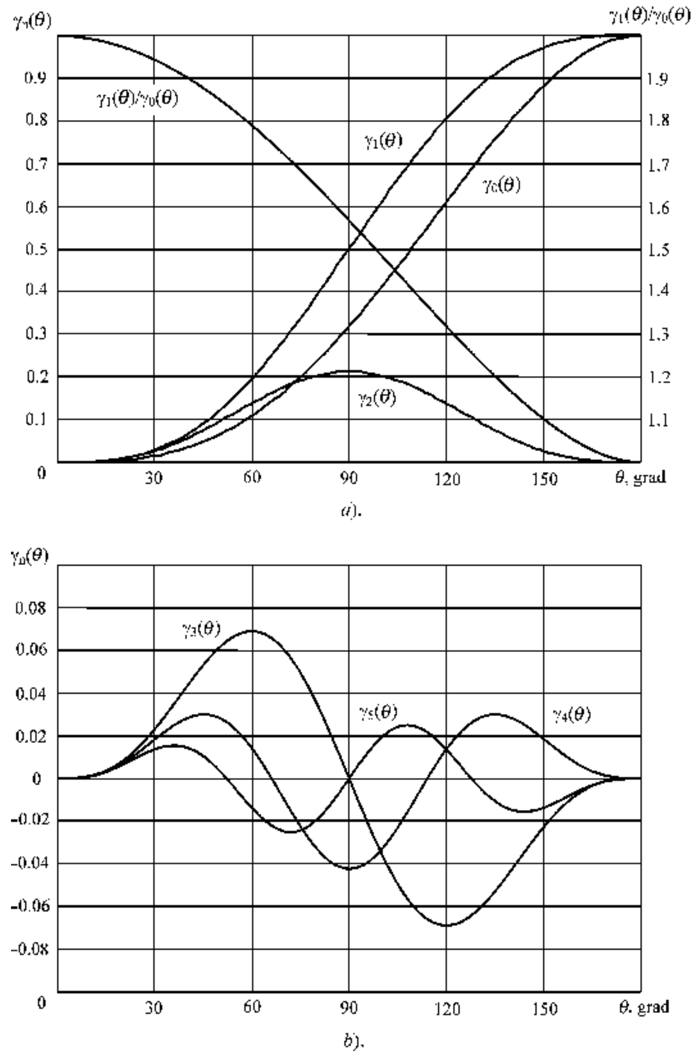

Figure 1.3 Dependencies of $\gamma_n(\theta)$ for dc, fundamental- and higher-order current components

$\gamma_n(\theta) > 0$ achieve positive maximum values at times corresponding to the midpoints of the current waveform, the harmonic components for which $\gamma_n(\theta) < 0$ can achieve negative maximum values at these times. As a result, combination of different harmonic components with proper loading will result in flattening of the current or voltage waveforms, thus improving efficiency of the oscillator. The amplitude of corresponding current harmonic component can be obtained as

$$I_n = \gamma_n(\theta) g_m V_{in} = \gamma_n(\theta) I \tag{1.28}$$

Sometimes it is necessary for an active device to provide a constant value of I_{max} at any value of θ. This requires an appropriate variation of the input voltage amplitude V_{in}. In this case, it is more convenient to use the other coefficients when the nth-order current harmonic amplitude I_n is related to the maximum current waveform amplitude $I_{\max}$, that is

$$\alpha_n = \frac{I_n}{I_{\max}} \tag{1.29}$$

From Equations (1.20), (1.28) and (1.29) it follows that

$$\alpha_n = \frac{\gamma_n(\theta)}{1 - \cos\theta} \tag{1.30}$$

and the maximum value of $\alpha_n(\theta)$ is achieved when $\theta = 120^\circ/n$.

1.1.3 Bessel functions

The Bessel functions are used to analyse the oscillator operation mode when a nonlinear behaviour of the active device can be described by exponential functions. The transfer voltage–ampere characteristic of the bipolar transistor is approximated by the simplified exponential dependence neglecting reverse base–emitter current as

$$i(v_{\text{in}}) = I_{\text{sat}}\left[\exp\left(\frac{v_{\text{in}}}{V_T}\right) - 1\right] \tag{1.31}$$

where I_{sat} is the minority carrier saturation current and V_T is the temperature voltage. If the effect of the input signal given by Equation (1.14) is considered, then Equation (1.31) can be rewritten as

$$i(\omega t) = I_{\text{sat}}\left[\exp\left(\frac{V_{\text{bias}}}{V_T}\right)\exp\left(\frac{V_{\text{in}}\cos\omega t}{V_T}\right) - 1\right] \tag{1.32}$$

The current $i(\omega t)$ in Equation (1.32) is the even function of ωt and, consequently, it can be represented by the Fourier-series expansion given by Equation (1.21). To determine the Fourier components, the following expression is used:

$$\exp\left(\frac{V_{\text{in}}\cos\omega t}{V_T}\right) = I_0\left(\frac{V_{\text{in}}}{V_T}\right) + 2\sum_{k=1}^{\infty} I_k\left(\frac{V_{\text{in}}}{V_T}\right)\cos(k\omega t) \tag{1.33}$$

where $I_k(V_{\text{in}}/V_T)$ are the kth-order modified Bessel functions of the first kind for an argument of V_{in}/V_T, shown in Figure 1.4 for the zeroth- and first-order components. It should be noted that $I_0(0) = 1$ and $I_1(0) = I_2(0) = \ldots = 0$, and with an increase of the component number its amplitude appropriately decreases.

According to Equation (1.33), the current $i(\omega t)$ defined by Equation (1.31) can be rewritten as

$$\begin{aligned} i(\omega t) = I_{\text{sat}}&\left[\exp\left(\frac{V_{\text{bias}}}{V_T}\right) I_0\left(\frac{V_{\text{in}}}{V_T}\right) - 1\right] + 2I_{\text{sat}}\exp\left(\frac{V_{\text{bias}}}{V_T}\right) I_1\left(\frac{V_{\text{in}}}{V_T}\right)\cos(\omega t) \\ &+ 2I_{\text{sat}}\exp\left(\frac{V_{\text{bias}}}{V_T}\right) I_2\left(\frac{V_{\text{in}}}{V_T}\right)\cos(2\omega t) + 2I_{\text{sat}}\exp\left(\frac{V_{\text{bias}}}{V_T}\right) I_3\left(\frac{V_{\text{in}}}{V_T}\right)\cos(3\omega t) + \ldots \end{aligned} \tag{1.34}$$

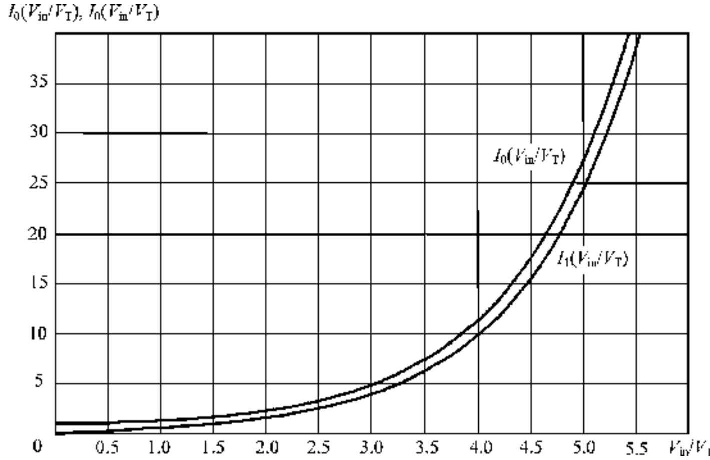

Figure 1.4 Zeroth- and first-order modified Bessel functions of the first kind

As a result, comparing Equations (1.34) and (1.21) allows the dc, fundamental-frequency and nth-order Fourier current components to be determined as

$$I_0 = I_{\text{sat}} \left[\exp\left(\frac{V_{\text{bias}}}{V_T}\right) I_0\left(\frac{V_{\text{in}}}{V_T}\right) - 1 \right] \tag{1.35}$$

$$I_1 = 2I_{\text{sat}} \exp\left(\frac{V_{\text{bias}}}{V_T}\right) I_1\left(\frac{V_{\text{in}}}{V_T}\right) \tag{1.36}$$

$$I_n = 2I_{\text{sat}} \exp\left(\frac{V_{\text{bias}}}{V_T}\right) I_n\left(\frac{V_{\text{in}}}{V_T}\right) \tag{1.37}$$

where $n = 2, 3, \ldots$.

When using the Bessel functions, the following relationships can be helpful:

$$2\frac{\mathrm{d}I_n\left(V_{\text{in}}/V_T\right)}{\mathrm{d}\left(V_{\text{in}}/V_T\right)} = I_{n+1}\left(\frac{V_{\text{in}}}{V_T}\right) + I_{n-1}\left(\frac{V_{\text{in}}}{V_T}\right) \tag{1.38}$$

$$\frac{\mathrm{d}I_0\left(V_{\text{in}}/V_T\right)}{\mathrm{d}\left(V_{\text{in}}/V_T\right)} = I_1\left(\frac{V_{\text{in}}}{V_T}\right) \tag{1.39}$$

$$\frac{2n}{\left(V_{\text{in}}/V_T\right)} I_{\text{n}}\left(\frac{V_{\text{in}}}{V_T}\right) = I_{n-1}\left(\frac{V_{\text{in}}}{V_T}\right) - I_{n+1}\left(\frac{V_{\text{in}}}{V_T}\right) \tag{1.40}$$

$$I_n\left(-\frac{V_{\text{in}}}{V_T}\right) = (-1)^n I_n\left(\frac{V_{\text{in}}}{V_T}\right) \tag{1.41}$$

1.2 TIME-DOMAIN ANALYSIS

A time-domain analysis establishes the relationships between voltage and current in each circuit element in the time domain when a system of equations is obtained, applying Kirchhoff's law to the circuit to be analysed. Normally, in a nonlinear circuit, such a system will be composed of nonlinear integrodifferential equations. The solution to this system can be found by applying numerical integration methods. Therefore, the choices of the time interval and the initial point are very important to provide a compromise between speed and accuracy of calculation; the smaller the interval, the smaller the error, but the number of points to be calculated for each period will be greater, which will make the calculation slower.

To analyse a nonlinear system in the time domain, it is necessary to know the voltage–current relationships for all circuit elements. For example, for linear resistance R, when the sinusoidal voltage applies and current are flowing through it, the voltage–current relationship in the time domain is given by

$$V = RI \tag{1.42}$$

where V is the voltage amplitude and I is the current amplitude.

For linear capacitance C

$$i(t) = \frac{\mathrm{d}q(t)}{\mathrm{d}t} = \frac{\mathrm{d}q}{\mathrm{d}v}\frac{\mathrm{d}v}{\mathrm{d}t} = C\frac{\mathrm{d}v}{\mathrm{d}t} \tag{1.43}$$

For linear inductance L

$$v(t) = \frac{\mathrm{d}\varphi(t)}{\mathrm{d}t} = \frac{\mathrm{d}\varphi}{\mathrm{d}i}\frac{\mathrm{d}i}{\mathrm{d}t} = L\frac{\mathrm{d}i}{\mathrm{d}t} \tag{1.44}$$

where φ is the magnetic flux across the inductance.

Nonlinear dependencies, such as $q(v)$ or $\varphi(i)$, should each be expanded in a Taylor series by subtracting the dc components and substituting into Equations (1.43) and (1.44) to obtain the expressions for appropriate incremental capacitance and inductance. Then, for the quasilinear case, the capacitance and inductance can be defined by

$$C(V_0) = \left.\frac{\mathrm{d}q(v)}{\mathrm{d}v}\right|_{v=V_0} \tag{1.45}$$

and

$$L(I_0) = \left.\frac{\mathrm{d}\varphi(i)}{\mathrm{d}i}\right|_{i=I_0} \tag{1.46}$$

where V_0 is the dc bias voltage across the capacitor and I_0 is the dc current flowing through the inductor.

Figure 1.5 shows the simplified (without bias circuits) electrical schematic of a transformer-coupled MOSFET oscillator with a parallel resonant circuit. To obtain the differential equations

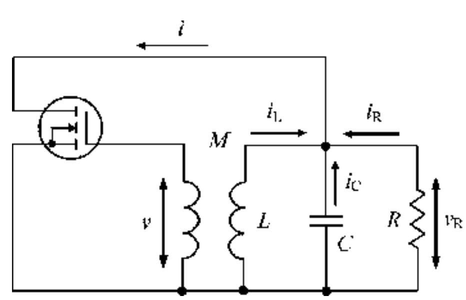

Figure 1.5 Schematic of a transformer-coupled MOSFET oscillator

for such an oscillator, the drain current i, the gate voltage v applied to the second winding of the transformer, and the load voltage v_R applied to the first winding of this transformer can be defined by

$$i = i_L + i_C + i_R \tag{1.47}$$

$$v_R = L\frac{di_L}{dt} = \frac{1}{C}\int i_C dt = i_R R \tag{1.48}$$

$$v = M\frac{di_L}{dt} = \frac{M}{L}v_R \tag{1.49}$$

where M is the transformer coupling factor.

To simplify the calculation, two preliminary assumptions can be used:

- the input current flowing to the gate terminal of the active device is negligible, enabling one to consider its input impedance as infinite;
- the effect of the output voltage v_R on the drain current i is ignored, i.e.,

$$i = f(v). \tag{1.50}$$

In this case, the derivative of current $i(v)$ with respect to time is written as

$$\frac{di}{dt} = \frac{di}{dv}\frac{dv}{dt} = g_m(v)\frac{dv}{dt} \tag{1.51}$$

where $g_m = di/dv$ is the small-signal transconductance of the device transfer characteristic given by Equation (1.50).

Substituting Equations (1.48) and (1.50) into Equation (1.47) gives

$$\frac{1}{L}\int v_R dt + C\frac{dv_R}{dt} + \frac{v_R}{R} = f(v) \tag{1.52}$$

Then, by differentiating Equation (1.52) and using Equations (1.49) and (1.51), we can write the second-order differential equation for the oscillator in the form

$$\frac{d^2v}{dt^2} + \frac{1}{C}\left[\frac{1}{R} - \frac{Mg_m(v)}{L}\right]\frac{dv}{dt} + \omega_0^2 v = 0 \tag{1.53}$$

where

$$\omega_0 = \frac{1}{\sqrt{LC}}$$

is the oscillator resonant frequency.

Equation (1.53) is a nonlinear equation because its second term depends on the unknown variable v. This nonlinearity is a result of the active device nonlinearity. From Equation (1.53), the start-up and steady-state oscillation conditions can be determined, as well as the particular features of the steady-state oscillations and oscillator transient response. To determine the start-up conditions, it is necessary to replace nonlinear Equation (1.53) by an appropriate linear one, with the linear small-signal transconductance g_m at the operating bias point. In this case, we are interested only in the result of the small deviation from an equilibrium point, whether the oscillations will grow or dissipate.

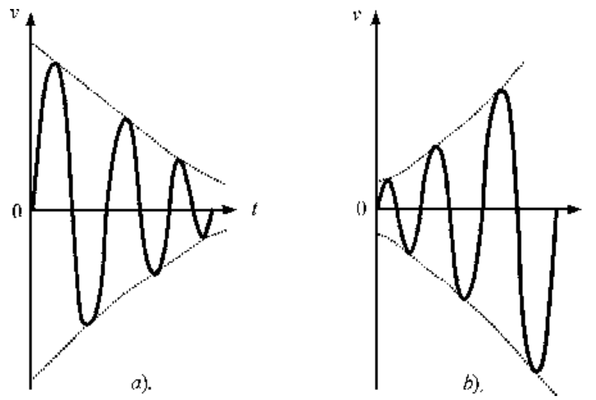

Figure 1.6 Oscillations with (a) low and (b) strong feedback factors

The solution of such a linear second-order differential equation is

$$v = V \exp(-\delta t) \sin(\omega_1 t + \phi) \tag{1.54}$$

where V and ϕ are the voltage amplitude and phase, respectively, depending on the initial conditions,

$$\delta = \frac{1}{2C}\left(\frac{1}{R} - \frac{M g_{\mathrm{m}}}{L}\right) \tag{1.55}$$

is the dissipation factor, and

$$\omega_1 = \sqrt{\omega_0^2 - \delta^2} \tag{1.56}$$

is the free-running oscillation frequency.

From Equation (1.54) it follows that the voltage v at the device input provided by the feedback circuit creates current i at the device output, which delivers electrical energy to the oscillation system to compensate for the losses in it. At the same time, the required value of this energy is the result of the transformation of the energy of the dc current delivered from the dc current source to the energy of the ac current. If the feedback factor is sufficiently small when $\delta > 0$, the delivered energy compensates for the dissipated energy only partly. As a result, this leads to attenuation and dissipation of the oscillations, as shown in Figure 1.6a. For strong feedback factor when $\delta < 0$, the delivered energy exceeds the dissipated energy, and the oscillations increase with time, as shown in Figure 1.6b.

1.3 NEWTON–RAPHSON ALGORITHM

To describe circuit behaviour, it is necessary to solve the nonlinear algebraic equation, or system of equations, which do not generally admit a closed form solution analytically. One of the most common numerical methods to solve such equations is a method based on the Newton–Raphson algorithm [2]. The initial guess for this method is chosen using a Taylor series expansion of the nonlinear function. Consider a practical case when the device is represented by a two-port network where all nonlinear elements are functions of the two unknown voltages, input voltage

v_{in} and output voltage v_{out}. As a result, after combining linear and nonlinear circuit elements, a system of two equations can be written as

$$f_1(v_{\text{in}}, v_{\text{out}}) = 0 \tag{1.57}$$

$$f_2(v_{\text{in}}, v_{\text{out}}) = 0 \tag{1.58}$$

Assume that the variables $v_{\text{in}0}$ and $v_{\text{out}0}$ are the initial approximate solution of a system of Equations (1.57) and (1.58). Then, the variables can be written as $v_{\text{in}} = v_{\text{in}0} + \Delta v_{\text{in}}$ and $v_{\text{out}} = v_{\text{out}0} + \Delta v_{\text{out}}$, where Δv_{in} and Δv_{out} are the linear increments of the variables. Applying a Taylor series expansion to Equations (1.57) and (1.58) yields

$$\begin{aligned} f_1(v_{\text{in}0} + \Delta v_{\text{in}}, v_{\text{out}0} + \Delta v_{\text{out}}) = {} & f_1(v_{\text{in}0}, v_{\text{out}0}) + \left.\frac{\partial f_1}{\partial v_{\text{in}}}\right|_{\substack{v_{\text{in}}=v_{\text{in}0} \\ v_{\text{out}}=v_{\text{out}0}}} \Delta v_{\text{in}} \\ & + \left.\frac{\partial f_1}{\partial v_{\text{out}}}\right|_{\substack{v_{\text{in}}=v_{\text{in}0} \\ v_{\text{out}}=v_{\text{out}0}}} \Delta v_{\text{out}} + o\left(\Delta v_{\text{in}}^2 + \Delta v_{\text{out}}^2 + \ldots\right) = 0 \end{aligned} \tag{1.59}$$

$$\begin{aligned} f_2\left(v_{\text{in}0} + \Delta v_{\text{in}}, v_{\text{out}0} + \Delta v_{\text{out}}\right) = {} & f_2\left(v_{\text{in}0}, v_{\text{out}0}\right) + \left.\frac{\partial f_2}{\partial v_{\text{in}}}\right|_{\substack{v_{\text{in}}=v_{\text{in}0} \\ v_{\text{out}}=v_{\text{out}0}}} \Delta v_{\text{in}} \\ & + \left.\frac{\partial f_2}{\partial v_{\text{out}}}\right|_{\substack{v_{\text{in}}=v_{\text{in}0} \\ v_{\text{out}}=v_{\text{out}0}}} \Delta v_{\text{out}} + o\left(\Delta v_{\text{in}}^2 + \Delta v_{\text{out}}^2 + \ldots\right) = 0 \end{aligned} \tag{1.60}$$

where $o(\Delta v_{\text{in}}^2 + \Delta v_{\text{out}}^2 + \ldots)$ denotes the second- and higher-order components.

By neglecting the second- and higher-order components, Equations (1.59) and (1.60) can be rewritten in matrix form

$$-\begin{bmatrix} f_1 \\ f_2 \end{bmatrix} = \begin{bmatrix} \dfrac{\partial f_1}{\partial v_{\text{in}}} & \dfrac{\partial f_1}{\partial v_{\text{out}}} \\ \dfrac{\partial f_2}{\partial v_{\text{in}}} & \dfrac{\partial f_2}{\partial v_{\text{out}}} \end{bmatrix} \begin{bmatrix} \Delta v_{\text{in}} \\ \Delta v_{\text{out}} \end{bmatrix} \tag{1.61}$$

In the phasor form,

$$-\boldsymbol{F} = \boldsymbol{J}\Delta\boldsymbol{v} \tag{1.62}$$

where $\boldsymbol{J}$ is the Jacobian matrix of a system of Equations (1.57) and (1.58).

The solution of Equation (1.62) for a nonsingular matrix $\boldsymbol{J}$ can be obtained by

$$\Delta\boldsymbol{v} = -\boldsymbol{J}^{-1}\boldsymbol{F} \tag{1.63}$$

This means that if

$$\boldsymbol{v}_0 = \begin{bmatrix} v_{\text{in}0} \\ v_{\text{out}0} \end{bmatrix} \tag{1.64}$$

is the initial guess of this system of equation, then the next (more precise) solution can be written as

$$\boldsymbol{v}_1 = \boldsymbol{v}_0 - \boldsymbol{J}^{-1}\boldsymbol{F} \tag{1.65}$$

where

$$\boldsymbol{v}_1 = \begin{bmatrix} v_{\text{in}1} \\ v_{\text{out}1} \end{bmatrix} \tag{1.66}$$

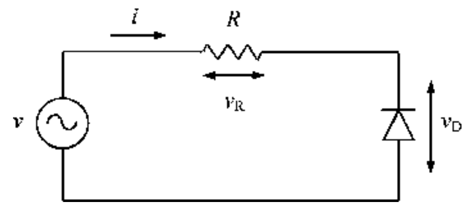

Figure 1.7 Circuit schematic with resistor, diode, and voltage source

Thus, starting with initial guess $\boldsymbol{v}_0$, we compute $\boldsymbol{v}_1$ at the first iteration. For the iteration $n + 1$, we can write

$$\boldsymbol{v}_{n+1} = \boldsymbol{v}_n - \boldsymbol{J}^{-1}\boldsymbol{F}(\boldsymbol{v}_n) \tag{1.67}$$

The iterative Equation (1.67) is given for a system of two equations; however it can be directly extended to a system of k nonlinear equations with k unknown parameters. This iterative procedure is terminated after $(n + 1)$ iterations whenever

$$|\boldsymbol{x}_{n+1} - \boldsymbol{x}_n| = \sqrt{\sum_{k=1}^{K} \left(x_{n+1}^k - x_n^k\right)^2} < \varepsilon \tag{1.68}$$

where ε is a small positive number depending on the desired accuracy. For a practical purpose, it is desirable that the Newton–Raphson algorithm should converge in a few steps. Therefore, the choice of an appropriate initial guess is crucial to the success of the algorithm.

Consider the circuit shown in Figure 1.7. According to Kirchhoff's voltage law,

$$v = v_{\mathrm{R}} + v_{\mathrm{D}} \tag{1.69}$$

where $v_{\mathrm{R}} = iR$.

The electrical behaviour of the diode is described by

$$i(v_{\mathrm{D}}) = I_{\mathrm{sat}}\left[\exp\left(\frac{v_{\mathrm{D}}}{V_T}\right) - 1\right] \tag{1.70}$$

Rearranging Equation (1.70) gives the equation for v_{D} in the form

$$v_{\mathrm{D}} = V_T \ln\left(\frac{i}{I_{\mathrm{sat}}} + 1\right) \tag{1.71}$$

Thus, from Equations (1.60) and (1.61) it follows that

$$v = iR + V_T \ln\left(\frac{i}{I_{\mathrm{sat}}} + 1\right) \tag{1.72}$$

This allows current i to be determined for a specified voltage v. However, because it is impossible to solve this equation analytically for current i in explicit form, the solution must be found numerically.

Consider a dc voltage source V with dc current I. For the sinusoidal voltage source, it is necessary to calculate the Bessel functions for dc, fundamental-frequency and higher-order

Table 1.1 Three-step iteration procedure

n	I_{n}, A	ε_{n}
0	0.05	0.899 371 786
1	0.878 469 005	0.070 902 781
2	0.948 955 229	0.000 416 557
3	0.949 371 786	

harmonic current components. It is convenient to rewrite Equation (1.72) as

$$f(I) = IR + V_T \ln\left(\frac{I}{I_{\mathrm{sat}}} + 1\right) - V = 0 \tag{1.73}$$

from which

$$f'(I) = R + \frac{V_T}{I + I_{\mathrm{sat}}} \tag{1.74}$$

Then, applying the iterative algorithm for a single variable, we can write

$$I_n = I_{n-1} - \frac{f\left(I_{n-1}\right)}{f'\left(I_{n-1}\right)}. \tag{1.75}$$

Using Equations (1.73) and (1.74) finally yields

$$I_n = I_{n-1} - \frac{I_{n-1}R + V_T \ln\left(\dfrac{I_{n-1}}{I_{\mathrm{sat}}} + 1\right) - V}{R + V_T \dfrac{1}{I_{n-1} + I_{\mathrm{sat}}}} \tag{1.76}$$

The results of the numerical calculation of the currents I_n for each iteration for $V_T =$ 25.9 mA/V, $R = 5\,\Omega$, $V = 5$ V, $I_{\mathrm{sat}} = 10$ μA and initial current $I_0 = 50$ mA are given in Table 1.1. The calculation error $\varepsilon_n = I_N - I_n$, where $n = 0, 1, \ldots, N$, illustrates the fast convergence to the solution for each iteration step. The error at each subsequent iteration step is approximately proportional to the square one of error at the previous step. If the required accuracy of $\varepsilon < 0.1\%$ is set in advance, the iteration procedure will be stopped at the third iteration step.

1.4 QUASILINEAR METHOD

To simplify the analysis and design procedure of the oscillator, in some cases it is enough to apply a quasilinear or Barkhausen–Moeller method based on the use of the ratios between the fundamental-frequency components of currents and voltages [3]. In this case, it is assumed that the self-oscillations must be close to sinusoidal. The derivation of equations for equivalent linear elements of the active device in terms of voltages and currents is based on its static voltage–ampere and voltage–capacitance characteristics.

For example, for a bipolar transistor, the simplified equivalent circuit of which is shown in Figure 1.8, all elements of its equivalent circuit are nonlinear, depending significantly on operation mode, especially the transconductance g_{m} and base-emitter capacitance C_π. The base-emitter capacitance C_π consists of the diffusion and junctions capacitances and, at

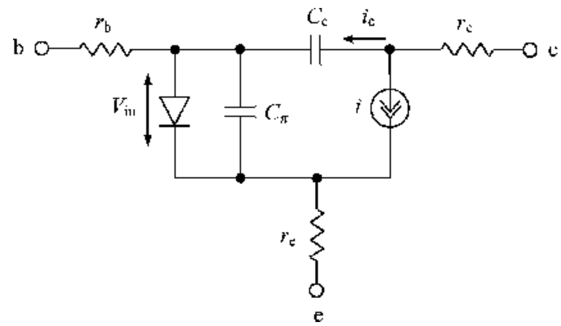

Figure 1.8 Bipolar transistor simplified equivalent circuit

high frequencies, its reactance is sufficiently high to shunt the base–emitter forward-biased diode. Taking into account that the transition frequency is obtained by $\omega_T = g_m/C_\pi$, it is sufficient to consider the only nonlinear elements g_m, ω_T and collector capacitance C_c, since the base resistance r_b poorly depends on a bias mode. The fundamentally averaged large-signal transconductance (or average transconductance) can be easily determined from Equation (1.36) by

$$g_{m1}(V_{in}) = \frac{I_1}{V_{in}} = \frac{2I_{sat}}{V_{in}} \exp\left(\frac{V_{bias}}{V_T}\right) I_1\left(\frac{V_{in}}{V_T}\right) \tag{1.77}$$

The collector capacitance C_c represents a junction capacitance and can be approximated by

$$C_c = \frac{C_{c0}}{\left(1 + \dfrac{v_c}{\varphi}\right)^\gamma} \tag{1.78}$$

where φ is the built-in junction potential, γ is the junction sensitivity and C_{c0} is the initial capacitance when $v_c = 0$.

If our interest is restricted to the fundamental frequency, and $v_c = V_{cc} + V_c \sin\omega t$, where V_{cc} is the collector dc supply voltage, then the following current flows through the collector capacitance which is defined for the quasilinear case as

$$\begin{aligned} i_c = C_c(v_c)\frac{dv_c}{dt} &= \frac{\omega C_{c0} V_c \cos\omega t}{\left(1 + \dfrac{V_{cc}}{\varphi} + \dfrac{V_c}{\varphi}\sin\omega t\right)^\gamma} \\ &= \frac{\omega C_c(V_{cc}) V_c \cos\omega t}{(1 + \xi\sin\omega t)^\gamma} \end{aligned} \tag{1.79}$$

where $C_c(V_{cc})$ is the small-signal capacitance in the operating point and $\xi = V_c/(V_{cc} + \varphi)$.

As a result, the average large-signal collector capacitance C_{c1} can be calculated through the fundamental Fourier series component as

$$C_{c1}(V_c) = \frac{I_{c1}}{\omega V_c} = \frac{C_c(V_{cc})}{\pi} \int_0^{2\pi} \frac{\cos^2\omega t}{(1 + \xi\sin\omega t)^\gamma} d(\omega t) \tag{1.80}$$

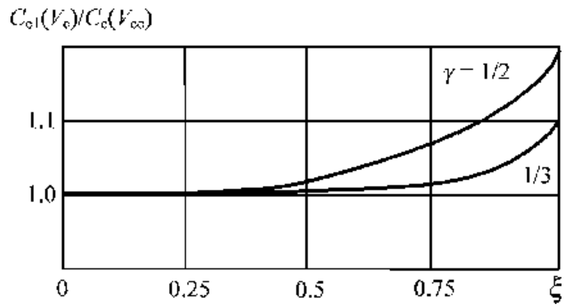

Figure 1.9 Large-signal behaviour of collector capacitance

Figure 1.9 shows the voltage dependencies of the average collector capacitance. Within a range of $\xi < 1$, the maximum large-signal value of $C_{c1}(V_c)$ deviates from the small-signal value of $C_c(V_{cc})$ by not more than 20% for an abrupt junction with $\gamma = 1/2$.

For a MESFET device with the simplified equivalent circuit shown in Figure 1.10, the drain current i_d is a function of the gate–source voltage v_{gs} and the drain–source voltage v_{ds}, which can be expanded in a two-dimensional Taylor series

$$i_d\left(v_{gs}, v_{ds}\right) = I_0 + \left.\frac{\partial f}{\partial v_{gs}}\right|_{\substack{v_{gs}=V_s \\ v_{ds}=V_{dd}}} (v_{gs} - V_g) + \left.\frac{\partial f}{\partial v_{ds}}\right|_{\substack{v_{gs}=V_g \\ v_{ds}=V_{dd}}} (v_{ds} - V_{dd})$$
$$+ \frac{1}{2}\left[\left.\frac{\partial^2 f}{\partial v_{gs}^2}\right|_{\substack{v_{gs}=V_g \\ v_{ds}=V_{dd}}} (v_{gs} - V_g)^2 + 2\left.\frac{\partial^2 f}{\partial v_{gs}\partial v_{ds}}\right|_{\substack{v_{gs}=V_g \\ v_{ds}=V_{dd}}} (v_{gs} - V_g)(v_{ds} - V_{dd})\right.$$
$$\left. + \left.\frac{\partial^2 f}{\partial v_{ds}^2}\right|_{\substack{v_{gs}=V_g \\ v_{ds}=V_{dd}}} (v_{ds} - V_{dd})^2 + \ldots\right] \tag{1.81}$$

where V_g is the gate dc bias voltage and V_{dd} is the drain dc supply voltage.

In the small-signal quasilinear case, the high-degree terms are neglected and

$$i_d(v_{gs}, v_{ds}) = I_0 + \left.\frac{\partial f}{\partial v_{gs}}\right|_{\substack{v_{gs}=V_g \\ v_{ds}=V_{dd}}} (v_{gs} - V_g) + \left.\frac{\partial f}{\partial v_{ds}}\right|_{\substack{v_{gs}=V_g \\ v_{ds}=V_{dd}}} (v_{ds} - V_{dd}) \tag{1.82}$$

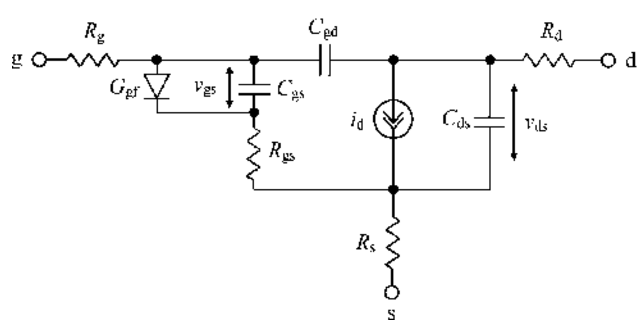

Figure 1.10 MESFET simplified equivalent circuit

The gate–source and drain–source instantaneous voltages can respectively be written as

$$v_{\mathrm{gs}} = V_{\mathrm{g}} + V_{\mathrm{gs}} \cos(\omega t + \phi) \tag{1.83}$$

$$v_{\mathrm{ds}} = V_{\mathrm{dd}} + V_{\mathrm{ds}} \cos \omega t \tag{1.84}$$

where V_{gs} and V_{ds} are the gate–source and drain–source voltage amplitudes and ϕ is the phase difference between these voltages.

Consequently, the instantaneous drain current given by Equation (1.81) can be rewritten as

$$i_{\mathrm{d}}(\omega t) = I_0 + g_{\mathrm{m1}} V_{\mathrm{gs}} \cos(\omega t + \phi) + G_{\mathrm{ds1}} V_{\mathrm{ds}} \cos \omega t \tag{1.85}$$

where

$$g_{\mathrm{m1}} = \left. \frac{I_{\mathrm{d}}}{V_{\mathrm{gs}}} \right|_{V_{\mathrm{ds}}=0} \tag{1.86}$$

is the linearized large-signal transconductance,

$$G_{\mathrm{ds1}} = \left. \frac{I_{\mathrm{d}}}{V_{\mathrm{ds}}} \right|_{V_{\mathrm{gs}}=0} \tag{1.87}$$

is the differential output conductance, I_0 is the dc drain current, I_{d} is the fundamental drain current amplitude, and $G_{\mathrm{ds1}} = 1/R_{\mathrm{ds1}}$ [4].

Multiplying the right- and left-hand sides of Equation (1.85) by $\sin \omega t$ and integrating over the entire period of the oscillation result in the average transconductance g_{m1} obtained by

$$g_{\mathrm{m1}} = -\frac{1}{\pi V_{\mathrm{gs}} \sin \phi} \int_0^{2\pi} i_{\mathrm{d}}(\omega t) \sin \omega t \, \mathrm{d}(\omega t) \tag{1.88}$$

Similarly, multiplying by $\sin(\omega t + \phi)$ results in the average output conductance

$$G_{\mathrm{ds1}} = \frac{1}{\pi V_{\mathrm{ds}} \sin \phi} \int_0^{2\pi} i_{\mathrm{d}}(\omega t) \sin(\omega t + \phi) \, \mathrm{d}(\omega t) \tag{1.89}$$

The average large-signal gate–source capacitance C_{gs1} can be calculated similarly to that of for the abrupt collector capacitance C_{c1} of the bipolar transistor with $\gamma = 1/2$. The average large-signal gate forward conductance G_{gf1} is defined by

$$G_{\mathrm{gf1}} = \frac{2I_{\mathrm{sat}}}{V_{\mathrm{gs}}} I_1 \left(\frac{V_{\mathrm{gs}}}{V_T} \right) \exp \left(\frac{V_{\mathrm{g}}}{V_T} \right) \tag{1.90}$$

where I_{sat} is the saturation current of the Schottky barrier, $I_1(V_{\mathrm{gs}}/V_T)$ is the first-order modified Bessel function of first kind.

The gate charging resistance R_{gs} varies with the gate–source capacitance C_{gs} in such a way that the charging time constant $\tau_{\mathrm{g}} = R_{\mathrm{gs}} C_{\mathrm{gs}}$ varies insignificantly and it can be treated as a constant in a quasilinear approximation.

Now consider the transient response which can be obtained using the quasilinear method on the example of the MOSFET oscillator, the simplified schematic of which is shown in Figure 1.5. For a quasilinear approximation, the appropriate ratios can be obtained directly from the nonlinear differential Equation (1.53) by substituting voltage v and current i by their fundamental-frequency components. The average transconductance g_{m1} is considered as a function of the slowly varying fundamental voltage amplitude and, for a high quality factor of the oscillator resonant circuit, can be treated constant during the natural oscillation period. As a result, the nonlinear differential Equation (1.53) can be considered as linear written in the form of

$$\frac{d^2 v}{dt^2} + \frac{1}{C}\left[\frac{1}{R} - \frac{M g_{m1}(V)}{L}\right]\frac{dv}{dt} + \omega_0^2 v = 0 \tag{1.91}$$

where V is the fundamental-frequency voltage amplitude.

From Equation (1.54) it follows that the amplitude of the oscillations varies according to

$$\frac{dV}{dt} = -\delta(V)V \tag{1.92}$$

where

$$\delta(V) = \frac{1}{2C}\left(\frac{1}{R} - \frac{M g_{m1}(V)}{L}\right)$$

Then, Equation (1.92) can be rewritten as

$$\frac{2}{\omega_0}\frac{dV}{dt} = \frac{1}{Q}\left(\frac{g_{m1}}{g_{m1}^0} - 1\right)V \tag{1.93}$$

where $Q = \omega_0 RC$ is the oscillator quality factor at the resonant frequency ω_0, and

$$g_{m1}^0 = \frac{L}{MR} \tag{1.94}$$

is the average transconductance in the steady-state oscillation mode.

The device voltage–ampere characteristic can be represented by a third-order power series given by Equation (1.3). Then, from Equation (1.10) it follows that

$$g_{m1}(V) = \frac{I_1}{V} = g_m - \frac{3}{4}g_{m3}V^2 \tag{1.95}$$

where $g_m = a_1$ is the small-signal transconductance at the operating bias point, $g_{m3} = -a_3$ and $a_1 > 0$, $a_3 < 0$ to provide soft start-up conditions.

Multiplying by V, separating variables and integrating the both parts of Equation (1.93) result in the amplitude transient response in the form

$$V = V_0 \Bigg/ \sqrt{1 + \left[\frac{V_0^2}{V^2(0)} - 1\right]\exp[-2|\delta(0)|t]} \tag{1.96}$$

where $V(0)$ is the amplitude V at $t = 0$, and

$$V_0 = \frac{2}{\sqrt{3g_{m3}}}\sqrt{g_m - g_{m1}^0} \tag{1.97}$$

is the voltage amplitude in the steady-state operation mode.

For the specified small-signal value of $\delta(0)$, the settling time of the oscillations will be defined by the ratio between the initial and steady state amplitudes. If $V(0) < V_0$, then the amplitude V increases monotonically, beginning with a small value $V(0)$ and nears the amplitude V_0, as shown in Figure 1.11. In this case, taking into account that at the beginning $V_0/V(0) \gg 1$ and neglecting the unit component in Equation (1.96), the amplitude increase

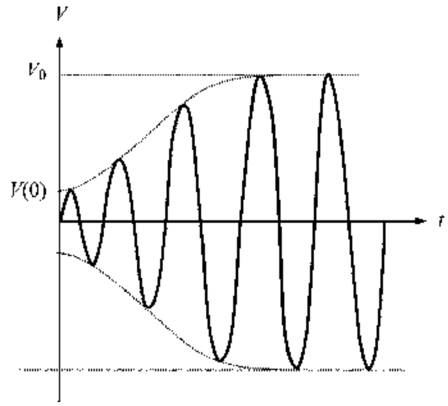

Figure 1.11 Transient response of transformer-coupled MOSFET oscillator

yields to an exponential law according to

$$V = V(0)\exp[|\delta(0)|t] \tag{1.98}$$

which gives, theoretically, an infinitely long settling time t_s.

Defining t_s as the time when the amplitude V increases up to $0.9V_0$, from Equation (1.96) we can obtain

$$t_s = \frac{1}{|\delta(0)|}\ln\left[\frac{2V_0}{V(0)}\right] \tag{1.99}$$

which means that an increase of the coupling factor M or small-signal transconductance g_m results in a shortening of the settling time. Hence, the settling time depends strongly on the initial amplitude $V(0)$ which is determined by the fluctuation process.

1.5 VAN DER POL METHOD

To illustrate a van der Pol method for analysing the behaviour of the oscillation systems described by the nonlinear second-order differential equations, let us consider once again the schematic of the transformer-coupled MOSFET oscillator shown in Figure 1.5. In this case, it is advisable to rewrite the nonlinear second-order differential equation given by Equation (1.53) in the form

$$\frac{d^2v}{dt^2} + 2\delta\frac{dv}{dt} + \omega_0^2 v = 2\delta R\frac{M}{L}\frac{di}{dt} \tag{1.100}$$

where the dissipation factor $\delta = 1/2RC$ includes only losses in the resonant circuit. Now we can use the method of slowly varying amplitudes (the van der Pol method) when Equation (1.100) is replaced by the corresponding truncated first-order differential equations for slowly varying amplitude and phase, respectively [3, 5, 6].

We shall seek a solution of Equation (1.100) in the form of the periodic oscillations of

$$v = V(t)\cos[\omega_0 t + \varphi(t)] \tag{1.101}$$

where $V(t)$ and $\varphi(t)$ are the slowly varying amplitude and phase, respectively. The term 'slowly varying' means that the relative variations of the amplitude and phase during the natural oscillation period are substantially smaller than unity. This means that the time derivatives of the amplitude and phase can be replaced by their average velocities during the oscillation period, i.e.,

$$\frac{dV}{dt} = \frac{\Delta V}{T} = \frac{\omega_0}{2\pi}\Delta V \tag{1.102}$$

$$\frac{d\varphi}{dt} = \frac{\Delta\varphi}{T} = \omega_0\frac{\Delta\varphi}{2\pi} \tag{1.103}$$

Then, under an assumption of slowly varying amplitude when $\Delta V/V \ll 1$, we can write

$$\frac{dV}{dt} \ll \omega_0 V \tag{1.104}$$

Accordingly, for higher-order derivatives of the voltage amplitudes, it is also assumed that

$$\frac{d^2V}{dt^2} \ll \omega_0\frac{dV}{dt} \qquad \frac{d^3V}{dt^3} \ll \omega_0\frac{d^2V}{dt^2} \qquad \ldots \tag{1.105}$$

Similarly, for the slowly varying phase when $\Delta\varphi/2\pi \ll 1$ and its higher-order derivatives, we can write

$$\frac{d\varphi}{dt} \ll \omega_0 \tag{1.106}$$

$$\frac{d^2\varphi}{dt^2} \ll \omega_0\frac{d\varphi}{dt} \qquad \frac{d^3\varphi}{dt^3} \ll \omega_0\frac{d^2\varphi}{dt^2} \qquad \ldots \tag{1.107}$$

The current $i(v)$ where v is defined by Equation (1.101) can be represented by a Fourier series

$$i(v) = I_0(V) + I_{1c}(V)\cos(\omega_0 t + \varphi) - I_{1s}(V)\sin(\omega_0 t + \varphi) + \ldots \tag{1.108}$$

where

$$I_{1c}(V) = \frac{1}{\pi}\int_{-\pi}^{\pi} i(V\cos\psi)\cos\psi\, d\psi \tag{1.109}$$

$$I_{1s}(V) = -\frac{1}{\pi}\int_{-\pi}^{\pi} i(V\cos\psi)\sin\psi\, d\psi \tag{1.110}$$

The first and second derivatives of Equation (1.101) can be calculated as

$$\frac{dv}{dt} = \frac{dV}{dt}\cos(\omega_0 t + \varphi) - V\left(\omega_0 + \frac{d\varphi}{dt}\right)\sin(\omega_0 t + \varphi) \tag{1.111}$$

$$\begin{aligned}\frac{d^2v}{dt^2} &= \frac{d^2V}{dt^2}\cos(\omega_0 t + \varphi) - 2\frac{dV}{dt}\left(\omega_0 + \frac{d\varphi}{dt}\right)\sin(\omega_0 t + \varphi)\\ &\quad + V\frac{d^2\varphi}{dt^2}\sin(\omega_0 t + \varphi) - V\left[\omega_0^2 + 2\omega_0\frac{d\varphi}{dt} + \left(\frac{d\varphi}{dt}\right)^2\right]\cos(\omega_0 t + \varphi)\end{aligned} \tag{1.112}$$

Equation (1.112) can be simplified by neglecting the terms with second derivatives and square of the first derivative to

$$\frac{\mathrm{d}^2 v}{\mathrm{d}t^2} = -2\omega_0 \frac{\mathrm{d}V}{\mathrm{d}t} \sin(\omega_0 t + \varphi) - \left(\omega_0^2 + 2\omega_0 \frac{\mathrm{d}\varphi}{\mathrm{d}t}\right) V \cos(\omega_0 t + \varphi) \tag{1.113}$$

Similarly, by taking into account only linear terms in Equation (1.108), the current derivative $\mathrm{d}i(v)/\mathrm{d}t$ can be obtained as

$$\begin{aligned}\frac{\mathrm{d}i(v)}{\mathrm{d}t} &= -I_{1c}(V)\left(\omega_0 + \frac{\mathrm{d}\varphi}{\mathrm{d}t}\right)\sin(\omega_0 t + \varphi) - \frac{\mathrm{d}I_{1c}(V)}{\mathrm{d}t}\cos(\omega_0 t + \varphi)\\ &\quad - I_{1s}(V)\left(\omega_0 + \frac{\mathrm{d}\varphi}{\mathrm{d}t}\right)\cos(\omega_0 t + \varphi) - \frac{\mathrm{d}I_{1s}(V)}{\mathrm{d}t}\sin(\omega_0 t + \varphi)\end{aligned} \tag{1.114}$$

As a result, for small values of the dissipation factor and derivatives of the slowly varying functions, Equation (1.100) can be rewritten using Equations (1.111), (1.113) and (1.114) as

$$\begin{aligned}&-2\omega_0 \frac{\mathrm{d}V}{\mathrm{d}t}\sin(\omega_0 t + \varphi) - 2\delta\omega_0 V \sin(\omega_0 t + \varphi) - 2\omega_0 V \frac{\mathrm{d}\varphi}{\mathrm{d}t}\cos(\omega_0 t + \varphi)\\ &\quad = -2\delta\omega_0 \frac{M}{L} R I_{1c}(V)\sin(\omega_0 t + \varphi) - 2\delta\omega_0 \frac{M}{L} R I_{1s}(V)\cos(\omega_0 t + \varphi)\end{aligned} \tag{1.115}$$

Finally, equating the terms with sinusoidal and cosinusoidal components in Equation (1.115) results in separate equations for the time-varying amplitude $V(t)$ and phase $\varphi(t)$ in the form

$$\frac{1}{\delta}\frac{\mathrm{d}V}{\mathrm{d}t} + V = \frac{M}{L} R I_{1c}(V) \tag{1.116}$$

$$\frac{1}{\delta} V \frac{\mathrm{d}\varphi}{\mathrm{d}t} = \frac{M}{L} R I_{1s}(V) \tag{1.117}$$

For the algebraic transfer function $i(v)$ and cosinusoidal input voltage v in Equation (1.101), the integral for $I_{1s}(V)$ given by Equation (1.110) is equal to zero. Physically this means that the active device has no reactive elements and the oscillator resonant frequency is fully defined by the resonant frequency ω_0 of the parallel *LC* circuit. Therefore, as follows from Equation (1.117), the phase $\varphi(t)$ of the oscillations given by Equation (1.101) is constant and no longer a function of time. At the same time, the amplitude of the oscillations, which behaviour is described by Equation (1.116), varies exponentially, depending on the dissipation factor δ. The similar result obtained by a quasilinear method is presented by Equation (1.92).

Generally, a procedure of the derivation of the truncated lower-order differential equations from the original nonlinear differential equations is very complicated and time-consuming, even for the simple cases. However, using a symbolic representation of the nonlinear oscillation behaviour and following a Evtyanov approach make it possible to speed up the procedure of obtaining the truncated equations [6, 7].

According to a Evtyanov approach, the oscillator can generally be represented by the ideal current source $i(v)$ and linear two-port network $Z(p)$, where $p \equiv \mathrm{d}/\mathrm{d}t$ is the differential operator, as shown in Figure 1.12. A symbolic equation to describe the behaviour of the oscillator is written as

$$v = Z(p)\, i(v) \tag{1.118}$$

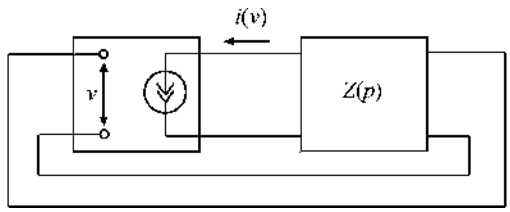

Figure 1.12 General oscillator model

where

$$Z(p) = \frac{\delta P(p,\delta)}{Q(p,\delta)} \tag{1.119}$$

$P(p, \delta)$ and $Q(p, \delta)$ are the polynomial functions of p and δ is the small parameter. For the oscillation systems with high quality factors, the small parameter δ usually represents a dissipation factor for one of its natural frequencies. The differential equation corresponding to a symbolic Equation (1.118) can be obtained by

$$Q(p,\delta)\, v = \delta P(p,\delta)\, i(v) \tag{1.120}$$

A solution of the differential Equation (1.120) is seeking a sum of the oscillations with the slowly varying amplitudes and phases according to

$$v = V_0(t) + \sum_{k=1}^{K} V_k(t) \cos[\omega_{0k} t + \varphi_k(t)] \tag{1.121}$$

where $k = 1, 2, \ldots, K$.

The complex voltage and current amplitudes can be written as

$$\boldsymbol{V}_k = V_k \exp(j\varphi_k) \tag{1.122}$$

$$\boldsymbol{I}_k = I_k \exp(j\varphi_k) \tag{1.123}$$

Then, using a two-dimensional Maclaurin series expansion about $p = 0, \delta = 0$ and neglecting the terms of order δ^2, the following system of truncated differential equations in a complex form can be obtained:

$$\left\{ \left(\frac{\partial Q(p,\delta)}{\partial p} \right]_k p + \left(\frac{\partial Q(p,\delta)}{\partial \delta} \right]_k \delta \right\} \boldsymbol{V}_k = \delta (P(p, \delta)]_k \boldsymbol{I}_k \tag{1.124}$$

Dividing both sides of Equation (1.124) by

$$\left(\frac{\partial Q(p,\delta)}{\partial \delta} \right]_k \delta$$

allows us to rewrite Equation (1.124) in the final form

$$(T_k p + 1)\, \boldsymbol{V}_k = Z_k \boldsymbol{I}_k \tag{1.125}$$

where

$$T_k = \left(\frac{\partial Q(p,\delta)}{\partial p}\right]_k \Big/ \delta \left(\frac{\partial Q(p,\delta)}{\partial \delta}\right]_k \tag{1.126}$$

$$\mathrm{Z}_k = (P(p,\delta)]_k \Big/ \left(\frac{\partial Q(p,\delta)}{\partial \delta}\right]_k \tag{1.127}$$

Substituting the complex voltage and current amplitudes from Equations (1.122) and (1.123) into Equation (1.125) and equating the real and imaginary parts after its differentiating result in two separate differential equations for amplitude and phase, respectively:

$$(T_k p + 1)V_k = R_k I_k(V_0, V_1, \ldots, V_K) \tag{1.128}$$

$$T_k V_k p\varphi_k = X_k I_k(V_0, V_1, \ldots, V_K) \tag{1.129}$$

where $R_k = \mathrm{Re}Z_k$, $X_k = \mathrm{Im}Z_k$, $k = 1, 2, \ldots, K$.

Comparison of a system of Equations (1.128) and (1.129) with a system of Equations (1.116) and (1.117) shows that these truncated differential equations for the slowly varying amplitude and phase are identical when $k = 1$, $V_0 = 0$ and $T_1 = 1/\delta$.

1.6 COMPUTER-AIDED ANALYSIS AND DESIGN

To analyse the nonlinear oscillator circuit, it is necessary to provide its frequency-domain and time-domain simulations giving the device, time, spectral or sweep presentations of the electrical characteristics and optimization of the circuit parameters to realize the optimum solution depending on customer requirements. The algorithm for nonlinear oscillator analysis used in Microwave Harmonica, which is a part of the Ansoft circuit simulator Serenade, is a modified harmonic balance method and can be divided into two steps: search and analysis [8, 9]. In the search mode, an external test source is added to an oscillator circuit to inject ac power, and forces the system away from the degenerate solutions when all ac currents are equal to zero is also a solution of Kirchhoff's current law. This approach includes the Kurokawa oscillation condition, which ensures that the degenerate solution is not obtained. The final steady-state solution of the search mode is treated as the initial estimate for the analysis mode. In the analysis mode, the system equation is solved using the modified harmonic balance method, in which oscillating frequency is used as an independent variable.

The search method includes the injection of an external ac source into the oscillator circuit and finding the steady-state operation mode using harmonic balance conditions and the Newton iteration scheme to solve a set of the system equations expressed in the frequency domain. By sweeping the injected frequency and power and examining both the magnitude and phase of the injected current, the oscillating condition of the circuit can be determined. The free-running oscillator is treated as a one-port network, as shown in Figure 1.13, where Y is the input admittance of overall one-port network including the load admittance Y_{L}, Y_{in} is the equivalent input admittance of the oscillator resonant circuit with the active device.

The steady-state condition for a single-oscillation frequency ω can be written as

$$Y = Y_{\mathrm{in}} + Y_{\mathrm{L}} = 0 \tag{1.130}$$

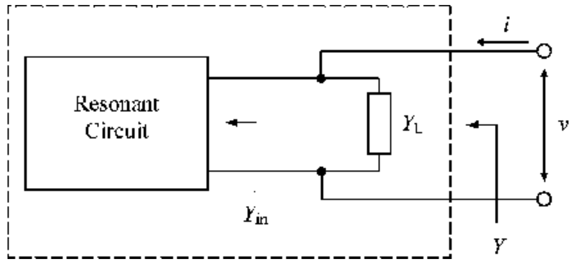

Figure 1.13 Application of the modified harmonic balance method to a free-running oscillator

which can be applied to each frequency component. Therefore, if K different frequency components ω_k are present, the oscillation conditions are determined by

$$Y_k = Y_{\text{in},k} + Y_{\text{L},k} = \text{Re}Y_k + j\text{Im}Y_k = 0 \tag{1.131}$$

where $k = 1, 2, \ldots, K$ indicates that the admittance Y_k is evaluated at each frequency ω_k.

As a result, if current $i(t)$ and voltage $v(t)$ are represented in the time domain by

$$i(t) = \sum_{k=0}^{K} i_k(t) = \sum_{k=0}^{K} I_k \cos(\omega_k t + \phi_k) \tag{1.132}$$

$$v(t) = \sum_{k=0}^{K} v_k(t) = \sum_{k=0}^{K} V_k \cos(\omega_k t + \theta_k) \tag{1.133}$$

where I_k and ϕ_k are the current amplitude and phase, V_k and θ_k are the voltage amplitude and phase, then the input admittance Y_k can be determined by phasor voltage $\boldsymbol{V}_k$ and phasor current $\boldsymbol{I}_k$ as

$$Y_k = \frac{\boldsymbol{I}_k}{\boldsymbol{V}_k} \tag{1.134}$$

By separating the real and imaginary parts of Y_k in Equation (1.131), we can obtain

$$\text{Re}Y_k = \text{Re}(\boldsymbol{I}_k/\boldsymbol{V}_k) = 0 \tag{1.135}$$

and

$$\text{Im}Y_k = \text{Im}(\boldsymbol{I}_k/\boldsymbol{V}_k) = 0 \tag{1.136}$$

which implies

$$\text{Re}I_k = \text{Im}I_k = 0 \tag{1.137}$$

and

$$V_k \neq 0 \tag{1.138}$$

The results obtained by Equations (1.135–1.138) show that, if the voltage amplitude of the injected test source in Figure 1.13 is large enough and the current amplitude of the test source under the harmonic balance condition is zero, the circuit is in oscillation condition. After changing the frequency and power of the external source and monitoring the injected current value, the oscillation condition of the test circuit can be determined. For an efficient search of the frequency and power of the external source when $k = 1$, the following algorithm has been used:

- the external power is set to be constant and at a low level;
- the frequency of the external source is swept until $\mathrm{Im}I_1$ is close to zero and $\mathrm{Re}I_1$ is negative;
- the power of the external source is increased stepwise and tracks the frequency until both $\mathrm{Re}I_1$ and $\mathrm{Im}I_1$ are close to zero.

When both $\mathrm{Re}I_1$ and $\mathrm{Im}I_1$ are reduced to very small values, highly accurate analysis results may be obtained. Furthermore, in order to avoid a large number of computations, a near target solution of about 0.1% error provides a good initial estimate for the analysis mode.

In the analysis mode, the external injected source is excluded and a modified harmonic balance technique is used to obtain a true and rigorous oscillator circuit analysis result. For a nonautonomous circuit analysis, the state variable vector $\boldsymbol{X}$ is composed of the state variables, including device port voltages, and error vector $\boldsymbol{E}$ is composed of the elements of the system errors, including corresponding port current errors. However, for the oscillator analysis, the structure of vector $\boldsymbol{X}$ is modified with the oscillating frequency f_1 as an additional variable, so the phases of the harmonic state variable voltages are referred to the phase of the voltage of the first state variable. In the same manner, to eliminate the degenerate solution, the error function vector $\boldsymbol{E}$ is reconstructed by replacing the error function elements at the fundamental frequency by a function designed to avoid the degenerate solution.

One of the main concerns in the oscillator circuit analysis is to improve the convergence property of the oscillator circuit simulation, especially when it is designed with high-Q resonant tank circuit. In this case, the system error near the oscillation frequency can be very large. Therefore, two techniques, (1) initial frequency setting and (2) fundamental frequency searching, have been used in the circuit simulator [8]:

1. All the node voltages and edge currents can be randomly initialized within a certain range that can reflect the practical level of the oscillator output power P_{out}. The oscillating frequency f_1 should be initialized as sufficiently close to the actual value of the fundamental frequency f, for example, within $0.1f \leq f_1 \leq 10f$.
2. Another way to improve the convergence ability is to first decrease the number of harmonics in order to simplify the error surface and gradually restore it to the desired value. This means a consecutive consideration of the analysis at the fundamental frequency, and then repeating it with the second-harmonic signal present. After obtaining the convergence with the third-harmonic signal present, the number of harmonics is then increased to the maximum number specified by user. This is very important to avoid aliasing when a small number of frequency components are taken into account.

The optimization procedure, which is crucial to provide fast and accurate circuit design by adjusting the values of certain circuit parameters, is based on an iterative process, in which the circuit is simulated to ascertain its electrical responses as compared with the optimization goals. Circuit parameters are adjusted to produce improved circuit responses. The optimization process continues until the selected number of iterations is completed or the optimization goal is achieved. Each goal gives rise to an error value that represents the discrepancy between the simulated circuit response and the appropriate goal limit. If the response satisfies the limits, then the error value is zero. Otherwise, the error value depends on the magnitude of the difference between the simulated response and the appropriate goal limit. In this case, the error function serves as a figure of merit during optimization procedure to select the best optimizable values. This error function value is a sum of the individual goal errors, which are weighted measures of the difference between the simulated circuit response and the desired response, as specified in the goal values. Weights are associated with each goal in order to allow the emphasis of certain goals over others. In a common case, the error function EF is defined by

$$\mathrm{EF} = \sum\nolimits_{\text{phrases}} \sum\nolimits_{\text{groups}} \sum\nolimits_{f} \left[\sum\nolimits_{i} (w_i e_i)/N_f \right] \tag{1.139}$$

where e_i is the error function contribution from the ith goal at one frequency, w_i is the weighting factor associated with the ith goal, N_f is the number of frequencies for the goal group containing e_i, $\sum_i$ means the summation over all optimization goals in a group, $\sum_f$ means the summation over all frequencies for which a group of goals is specified, $\sum_{\text{groups}}$ means the summation over all groups and $\sum_{\text{phrases}}$ means the summation over all optimization phrases [9]. Each line of goals is considered as a group and may contain only one frequency range, at which all the goals in the group are evaluated, whereas a number of goal groups may be defined within each optimization phrase.

The optimization procedure may include different optimization methods, for example, several such methods as random search, gradient search and minimax search are used in Ansoft circuit simulator Serenade. The *gradient search* is based on a quasi-Newton algorithm, which uses the exact gradient and approximate inverse of the Hessian matrix of the error function to find a direction of improvement for each optimization value. The first search direction is in the direction of the gradient vector along a line in n-dimensional space where n is the number of optimized values. Once a minimum is found in the first direction, a second search along another line in the same n-dimensional space is performed. In the second and subsequent iterations, the direction of search depends on the gradient vector, which is not the same as the overall gradient. The direction of search is modified to accelerate convergence as a minimum is approached. However, the gradient search is susceptible to local minimum points when, once a local minimum region of the error function is reached, the gradient search method may have difficulty in selecting optimizable values outside that minimal region.

The *random search* selects new optimizable values following a Monte Carlo approach. Starting from an initial set of optimizable values, for which the error function value is known, a new set of values is obtained using a random-number generator within the applicable optimizable value ranges. The error function is re-evaluated and these optimizable values are retained if a decrease in its value is identified. This is a trial-and-error process, in which random search, step-by-step, finds at least minimum of the error function. The random search repeats this procedure for as many times as the number of iterations specified before the optimization is started in order to approximate to the global minimum of the error function as close as possible. Initially, new optimizable values are drawn according to a uniform Gaussian distribution for each optimizable value and these optimizable variables are treated as independent Gaussian variables. After each iteration, whether it is successive or not, the distribution is modified and becomes non-Gaussian to its skewing towards lower error function values and away from higher ones. The random search tends to proceed in the direction of error function reduction, but it is not restricted to such areas completely, allowing improvement of the search efficiency without the risk of trapping the search in local minimum.

The *minimax method* provides the minimization of the largest weighted goal errors, i.e., the minimization of the maximum contributions to the error function value. The minimax error function always represents only the worst case violation of the optimization goals, where the desired circuit response specifications are either most severely violated when EF > 0, or satisfied with the smallest margin when EF < 0. In this case, the error function to be minimized may be defined in general as

$$\mathrm{EF} = \mathrm{MAX}_{\mathrm{phrases}}\ \mathrm{MAX}_{\mathrm{groups}}\ \mathrm{MAX}_{f}\ \mathrm{MAX}_{\mathrm{goals}}(w_i e_i) \tag{1.140}$$

where e_i is the discrete error function associated with a phrase at one frequency, w_i is the weighting factor associated with e_i, $\mathrm{MAX}_{\mathrm{goals}}$ means maximum value in the set over all goals of a phrase, MAX_f means maximum value in the set over all frequencies of a group, $\mathrm{MAX}_{\mathrm{groups}}$ means maximum value over all goal groups and $\mathrm{MAX}_{\mathrm{phrases}}$ means maximum value over all optimization phrases. A minimax solution means that the goal specifications are met in an optimal, typically equal-ripple manner. The sophisticated minimax search method proceeds in two stages. In the first stage of the search, the minimax problem is solved using a linear programming technique and, in the second stage, the search employs a quasi-Newton algorithm with second-order derivatives. A minimax iteration requires one evaluation of the objective function and its gradient and therefore is less time-consuming than an iteration of the gradient search.

REFERENCES

1. A. I. Berg, *Theory and Design of Tube Generators* (in Russian), Moskva: GEI (1932).
2. J. K Fidler and C. Nightingale, *Computer Aided Circuit Analysis*, Middlesex: Thomas Nelson & Sons (1978).
3. A. A. Andronov, A. A. Vitt and S. E. Khaikin, *Theory of Oscillations*, New York: Dover Publications (1987).
4. Y. Tajima, B. Wrona and K. Mishima, ‘GaAs FET Large-Signal Model and its Application to Circuit Designs’, *IEEE Trans. Electron Devices*, **ED-28**, 171–175 (1981).
5. B. van der Pol, ‘The Nonlinear Theory of Electric Oscillations’, *Proc. IRE*, **22**, 1051–1086 (1934).
6. M. V. Kapranov, V. N. Kuleshov and G. M. Utkin, *Theory of Oscillations in Radio Engineering* (in Russian), Moskva: Nauka (1984).
7. S. I. Evtyanov, *Electron Tube Oscillators* (in Russian), Moskva: Svyaz (1967).
8. C. R. Chang, M. B. Steer, S. Martin and E. Reese, ‘Computer-Aided Analysis of Free-Running Microwave Oscillators’, *IEEE Trans. Microwave Theory Tech.*, **MTT-39**, 1735–1745 (1991).
9. Microwave Harmonica®, *Reference Volume*, *Version 7.5 P.C.*, Ansoft Corporation (1998).